Efficient Capacitance Solver for 3D Interconnect Based on Template-Instantiated Basis Functions

Yu-Chung Hsiao [yuchsiao@mit.edu],   Tarek El-Moselhy [tmoselhy@mit.edu],   Luca Daniel [luca@mit.edu]

Massachusetts Institute of Technology

Abstract

In this paper we show how the highly restrictive design rules of the recent sub-micro to nano-scale Integrated Circuit technologies allow to use a limited number of pre-computed surface charge distributions as a set of fundamental template basis functions in an efficient integral equation based 3D capacitance solver. Several examples verify that our solver can achieve final accuracies of less than 2% using 5× to 30× fewer unknowns than standard piecewise constant basis functions for the same accuracy, resulting in up to 25× speedups.

I. INTRODUCTION

The state-of-the-art in efficient capacitance extraction methods for integrated circuits involves 2D cross section scanning, determining wire adjacency, calculating 2D capacitance in a table lookup approach, and then reconstructing quasi-3D capacitance. Such approach is indeed fast, yet it is accurate only for 2D structures. Full 3D structures (e.g. crossing wires in adjacent metal layers) need the accuracy of electrostatic field solvers such as [1]–[4]. The most efficient of such tools are based on solving integral equations using piece-wise constant basis functions combined with standard collocation testing and iterative techniques. Such solvers are typically accelerated by fast matrix-vector products, which have a significant computational overhead, but scale almost linearly with the number of conductors. Hence they are ideal for very large scale examples.

On the other hand, improving time and memory requirements by the use of higher order basis functions such as piece-wise linear and quadratic bases is a common practice in almost all numerical communities when solving differential and integral equations. Sometimes even more efficient solvers are obtained by employing or developing specialized basis functions with "built-in" known physical properties such as sinusoidal bases for high frequency resonating antenna problems [5], loop-star bases for diverge-free unknowns [6], conduction mode bases for Helmholtz current distributions inside conductors [7]–[11], and edge and corner bases for surface charge density in capacitance extraction problems for microelectromechanical devices [12].

As in [12], this paper investigates the use of specialized basis functions to represent effectively the surface charge density distributions in integral equation based capacitance extraction solvers. However, the key idea in this paper is to exploit the charge distributions properties due to the highly restrictive design rules of the recent sub-micro to nano-scale integrated circuit and packaging technologies, as highlighted in Section III-A. As we will demonstrate in the example session, in this scenario the edge and corner bases introduced in [12] are not required to achieved accuracies of about 5%, typically required by integrated circuit and packaging applications. On the other hand, charge distributions and fringing fields induced by adjacent crossing wires, when neglected, can easily generate unacceptable errors in the 20% range. Pre-computed surface charge distributions shapes (defined in Section III-B) will be used in this work as specialized basis functions (Section III-C) to represent such induced charge distributions. A similar idea was introduced in [9] for proximity effect induced *currents*, as opposed to *charges*. An additional difference in this work is the idea of assembling the basis functions a priori and "on the fly" from just two basic building blocks. In this way analytical formulas and numerical tabulation of the Galerkin coefficients for our limited number of template building blocks can effectively limit the setup overhead as shown in Section III-D, obtaining fast simulation times and affordable memory requirements as demonstrated in the examples in Section IV.

II. BACKGROUND

A standard way to extract the capacitance matrix for a n-conductor system embedded in a uniform medium with dielectric constant ε is to solve the integral equation

$$\int_S \frac{\rho(\mathbf{r}')}{4\pi\varepsilon\|\mathbf{r} - \mathbf{r}'\|}d\mathbf{r}' = \Phi(\mathbf{r}) \tag{1}$$

for the surface charge density ρ, given the electric potential $\Phi(\mathbf{r})$. By expressing the charge density $\rho(\mathbf{r}') = \Sigma_j \rho_j \psi_j(\mathbf{r}')$ in a linear combination of N basis functions ψ_j and by using the standard Galerkin testing method, (1) becomes

$$\left[\int_{Si} \int_{Sj} \frac{\psi_i(\mathbf{r})\psi_j(\mathbf{r}')}{4\pi\varepsilon\|\mathbf{r} - \mathbf{r}'\|}d\mathbf{r}'d\mathbf{r} \right] \rho_j = \int_{Si} \psi_i(\mathbf{r})\Phi(\mathbf{r})d\mathbf{r} \tag{2}$$

where the integration in the brackets forms a system matrix, and ρ_j is a vector of N unknowns corresponding to each basis function.
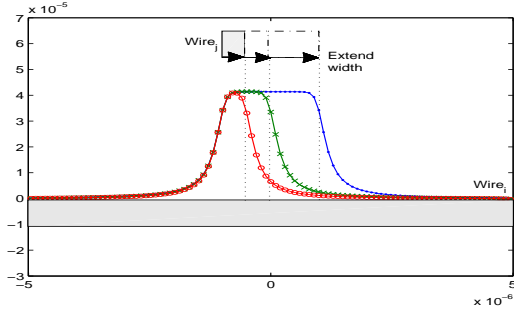
(a) The shape and slope of the induced charge density (cross-section) of the bottom wire are not affected by the width of the crossing wire.
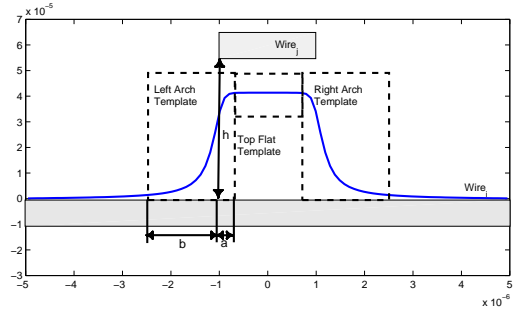
(b) Basis function instantiation and assembly process: a single basis is constructed connecting one flat and two arch templates.

Fig. 1. Capturing charge density induced by crossing wires.

III. TEMPLATE INSTANTIATED BASIS FUNCTIONS

A. Observed Charge Density Properties for Typical IC Interconnect

One key observation is that the surface charges accumulating on conductor corners and edges, as well as the charges induced on a conductor surface due to a nearby conductor, in typical IC interconnect geometries are generally quite confined. A second key observation is that corner and edge charge accumulations affect the wire capacitances by no more than a few percent, and therefore can be safely ignored for typical IC target accuracies of about 5%, as the first example in Section IV will verify. A third key observation is that the shape and slope of the charge density induced by a nearby wire is the same regardless of the width of the crossing wire as seen on Fig. 1(a). From the above observations, one can conclude that in order to represent most, if not all, charge distribution scenarios in IC/package applications, specialized basis functions can be easily instantiated a-priori from a very small number of pre-defined templates as shown for instance in Fig 1(b) for the two crossing wires, and as described in more details for other cases in Section III-C below. One can further conclude that given the small number of template building blocks, the coefficients of the Galerkin system matrix in eq. (2), representing the interaction between different bases, can be either tabulated and retrieved very efficiently, or computed partially analytically as shown in Section III-D, therefore avoiding expensive setup costs.

B. Definition of Charge Density Building Block Templates

We first define two simple 1D shape templates as follows:
- "Flat curve" template: $T_F(\cdot) = 1$, a 1D constant function.
- "Arch shape" template: $T_A(\cdot, a, b, h)$, a family of 1D decaying functions. Arch templates are characterized by the three parameters (a, b, h) defined in Fig. 1(b).

Using the two 1D template shapes above we define 2D building blocks:
- "Flat Building Block" : $B_F(u, v) = T_F(u) \cdot T_F(v)$,
- "Arch Building Block" : $B_{A,u\pm}(u, v) = T_A(\pm u) \cdot T_F(v)$ or $B_{A,u\pm}(u, v) = T_A(\pm v) \cdot T_F(u)$, for decaying in $\pm u$ and $\pm v$ directions, respectively,

where (u, v) are local coordinates on each conductor face. In our original formulation we had defined other building blocks such as corner and edge templates [12] shown in Fig. 3(b) and other blocks such as $T_A(\pm u) \cdot T_A(\pm v)$. In our experimentations we have however made the critical observation that only the Flat and Arch building blocks defined above are essential and sufficient to achieve the target 5% accuracies of typical IC capacitance extraction.
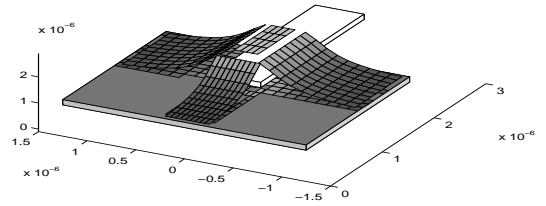
C. Instantiation and Assembly of Charge Density Basis Functions from Building Block Templates

Fig. 1(b) shows an example of the instantiation and assembly process for a basis function solely responsible to capture local charge accumulation induced on the bottom conductor by a nearby crossing conductor. A left arch building block, a right arch building block, and a flat building block are first instantiated to fit the appropriate dimensions of the neighboring wires. The three blocks are then connected together to constitute a *single* basis function, hence they will contribute to a single unknown in the final system (2). Each additional crossing wire will contribute a single extra basis function to the bottom conductor, hence contributing a single extra unknown to the system.

Another typical example of such instantiation and assembly process is illustrated in Fig 2(b) which shows one single basis function constructed on the fly by the solver by instantiating and connecting three arch building blocks and one flat building block in order to fit the wire dimensions shown in Fig. 2(a). The total number of basis functions used to represent the charge density of all surfaces of the bottom conductor is 7, i.e. one flat basis covering completely each face of each conductor, plus
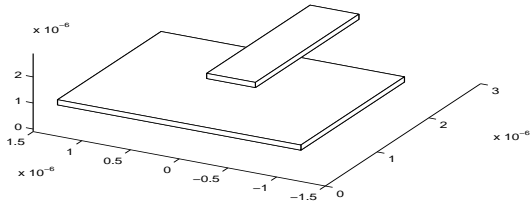
(a) Wires' geometry.

(b) The single basis function representing the induced charge density is assembled using three arch building blocks and one flat building block.

Fig. 2. Instantiation and assembly process for partially overlapping wires

the basis function shown in Fig. 2(b). One can notice how additional building blocks of the form $T_A(\pm u) \cdot T_A(\pm v)$ could have been used to capture corner fringe. However as mentioned multiple times the simple basis function as shown in Fig. 2(b) is necessary and sufficient for the target 5% accuracy of this problem.

A simple algorithm implementing the ideas illustrated in the two examples above has been developed (and cannot be included because of space limitations) to instantiate and assemble basis functions from our two building blocks for any given collection of wires in a Manhattan layout with rectangular wires.

D. Efficient System Matrix Assembly

In order to reduce the time required to calculate the Galerkin integrals for each of the system entry in eq. (2), we adopt a partially numerical - partially analytical scheme, summarized in Table below. In order to further increase efficiency we truncate and use a piecewise linear approximation for the arch shape.

| Building Block Interaction Type	Integration Schemes
Flat with *Flat*	3D analytical and 1D numerical
Flat with *Arch*	3D analytical and 1D numerical
Arch with *Arch* (different directions)	2D analytical and 2D numerical
Arch with *Arch* (same direction)	Summation of *Flat* with *Arch*

IV. EXAMPLES

Figure 3(a) shows the parametric sweep of aspect ratio and area for a single conductor solved using only one single flat basis function over each face, combined with the standard Galerkin testing approach. This simple setup achieves less than 3% relative error. Including additional basis functions representing edge and corner singularities [12] as shown in Fig. 3(b) achieves a significantly smaller relative error of 10^{-3}%. This example however demonstrates that for the 5% accuracy required by integrated circuit designs, edge and corner basis functions do not need to be included.

In the Table below we summarize the performance of several examples where we used the basis functions described in Section III-C with a standard Galerkin testing, and we compare them to piecewise constant (PWC) basis with collocation testing in uniform discretization. In both methods, systems are solved by standard Gaussian elimination. All our examples have been run in Matlab on a desktop computer with a Xeon 2.93GHz CPU.

| Example	Partially overlapping wires Fig. 2(a)			7 by 7 buses Fig. 4(a)			Routing wires between modules Fig. 4(b)		
Relative Error	1.6%			2.1%			1.7%		
	This work	PWC	Improvement	This work	PWC	Improvement	This work	PWC	Improvement
Unknown Number	17	572	33×	966	4688	4.8×	120	1754	14.6×
Filling Time (sec)	0.03s	0.75s	25×	14.1s	13.3s	0.94×	0.35s	1.9s	5.4×
Solving Time (sec)	< 0.1ms	0.015s	> 150×	0.05s	3.3s	60.7×	< 1ms	0.24s	> 240×
Total Time (sec)	0.03s	0.76s	25.3×	14.2s	16.6s	1.2×	0.35s	2.2s	6.1×
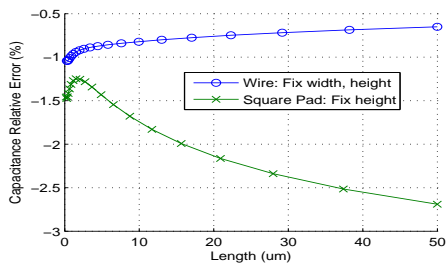
(a) Parametric sweep for capacitance error neglecting edge, corner singularity basis functions
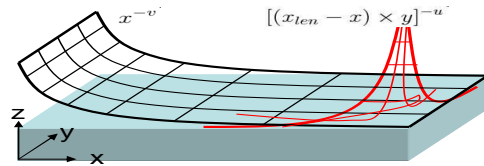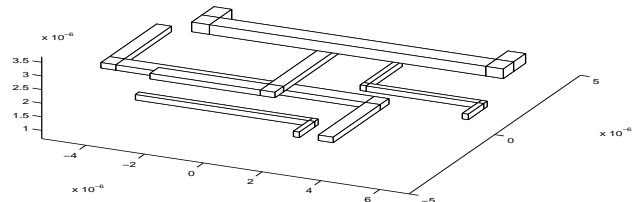

(b) Edge and corner singularity basis functions

Fig. 3.   Verification for neglecting singularity basis functions
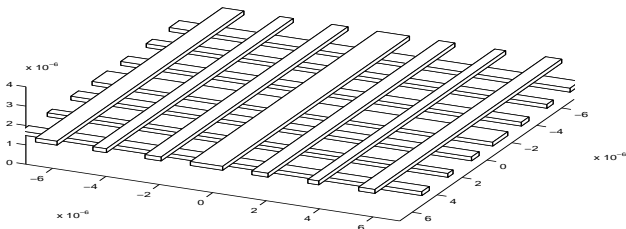
(a) 7 by 7 crossing bus example

(b) Routing wires between modules

Fig. 4.   Two larger examples

V. CONCLUSIONS

In this paper we have presented an integral equation based capacitance solver which instatiates on the fly a small number of specialized basis functions to capture charge distributions induced by nearby conductors. In a medium size example, our solver used a total of just 120 unknowns, obtaining a worst-case relative error less than 2% compared to the result extracted by piecewise constant basis in a very fine discretization with tens of thousands of unknowns. Furthermore, the piecewise constant basis method requires 1754 unknowns to produce the same 2% error in a coarser discretization. Hence, for the same 2% accuracy, our algorithm requires approximately $14.6\times$ fewer unknowns, resulting in an overall $6\times$ speedup.

ACKNOWLEDGMENT

REFERENCES

[1] K. Nabors, J. K. White, "FASTCAP A multipole-accelerated 3D capacitance extraction program" *IEEE Transactions on Computer-Aided Design of Integrated Circuits and Systems*, pp. 1447–1459, 1991.

[2] R. B. Iverson, Y. L. Le Coz, "A Stochastic Algorithm for High Speed capacitance Extraction in Integrated Circuits," *Solid-State Electronics*, Vol. 35, No. 7, pp. 1005–1012, 1992.

[3] J. R. Phillips, J. K. White, "A precorrected-FFT method for electrostatic analysis of complicated 3D structures" *IEEE Transactions on Computer-Aided Design of Integrated Circuits and Systems*, pp. 1059–1072, 1997.

[4] S. Kapur, D. Long, "IES3: Efficient Electrostatic and Electromagnetic Simulation" *IEEE Computational Science & Engineering*, pp. 60 – 67, 1998.

[5] W. A. Imbriale, "On numerical convergence of moment solutions of moderately thick wire antennas using sinusoidal basis functions", *IEEE Transactions on Antennas and Propagation*, v Ap-21, n 3, p 363-6, May 1973.

[6] "Loop-Star Decomposition of Basis Functions in the Discretization of the EFIE", *IEEE Trans. on Antennas and Propagation* Vol. 47, No. 2, Feb 1999.

[7] P. Silvester, "Model network theory of skin effect in flat conductors", *Proceedings of IEEE*, 54(9):1147-1151, September 1966.

[8] L. Daniel, A. Sangiovanni-Vincentelli, J. White, "Interconnect Electromagnetic Modeling using Conduction Modes as Global Basis Functions", *IEEE 9th Topical Meeting on Electrical Performance of Electronic Packaging*, 2000.

[9] L. Daniel, A. Sangiovanni-Vincentelli, J. White,"Proximity Templates for Modeling of Skin and Proximity Effects on Packages and High Frequency Interconnect", *IEEE/ACM International Conference on Computer Aided Design*, San Jose, Nov 2002.

[10] S. Ortiz, R. Suaya, "Fullwave volumetric Maxwell solver using conduction modes", *IEEE/ACM International Conference on Computer-Aided Design*, 2006.

[11] K.J. Han, E.Engin, M. Swaminathan, "Cylindrical Conduction Mode Basis Functions for Modeling of Inductive Couplings in System-in-Package (SiP)", *IEEE Topical Meeting on Electrical Performance of Eletronic Packaging*, 2007.

[12] Y. Su, E. T. Ong, K H Lee, "Automatic classification of singular elements for the electrostatic analysis of microelectromechical systems", *Journal of Mecromechanics and Microengineering*, Vol 12, pp.307-315, 2002.